Skin Surface Topographic Assessment using in vivo High-Definition Optical Coherence Tomography

Ai Ping Yow, Jun Cheng, Annan Li, Carolin Wall, Damon Wing Kee Wong and Jiang Liu
Institute for Infocomm Research, A*STAR
Singapore
E-mail: {yowap, jcheng, lia, stucw, wkwong, jliu} @ i2r.a-star.edu.sg

Hong Liang Tey
National Skin Centre
Singapore
E-mail: hltey@nsc.gov.sg

***Abstract*— Skin surface topography and wrinkles are important biophysical features in both dermatological and cosmeceutical practice and research. Current skin surface topography evaluation techniques, such as replica-based methods, have limitations which may result in errors and inaccurate measurement. High-Definition Optical Coherence Tomography (HD-OCT) is a recently-developed non-invasive skin imaging modality used clinically for visualizing skin structures. In this present work, we developed an automatic evaluation system to quantify the skin surface topography and wrinkles in HD-OCT images. Comparison of this system with subjective evaluations of skin surface roughness was carried out, and there was a good correlation between the results of these two methods of evaluation.**

I. INTRODUCTION

The skin is the outer covering of our body and is the largest organ of the integumentary system. Skin characteristics can vary due to numerous factors [1, 2] such as malignancy, aging, cosmetics and personal care products. Hence, the evaluation of the human skin surface topography is of particular importance to both dermatological and cosmeceutical practice and research. The irregularities in skin surface topography constitute roughness and wrinkles observed by the human eye. Skin surface roughness and wrinkles is an important evaluation item in evidence reports on the progress of dermatological treatment.

In most clinical settings, skin surface roughness and wrinkles are primarily assessed by visual inspection, with a critical dependence on clinicians' experiences. Besides visual inspection, roughness and wrinkles can also be quantitatively measured indirectly from skin replicas [3] which are produced by imprinting the skin surface onto a silicone material. Roughness measurement is then performed on the skin replicas using mechanical profilometry approach or optical techniques such as microphotography. However, replica-based methods are inconvenient in clinical settings and susceptible to distortions (including the presence of air bubbles) during skin relief reproduction, and require long scanning times [1]. Hence, direct in vivo methods are preferable. The technique widely used today for in vivo skin analysis is fringe projection area topography [3]. Examples of such area topography systems commercially available on the market include PRIMOS® and DermaTOP®. Despite having a fast acquisition time of less than 1 second, the drawbacks of such fringe projection methods are the interference of back scattering from skin tissue volume effects, the deformation of fringe image caused by micro body movement and the low accuracy due to a moderate resolution of 15-24µm [3].

With recent advances in imaging technology, the widespread use of imaging in clinics for skin surface evaluation is becoming a possibility. Optical Coherence Tomography (OCT) is a proven non-invasive technique for skin imaging [4] and recently, high-definition OCT (HD-OCT) is available with an enhanced resolution of 3µm in both axial and en face planes, allowing better visualization of skin structure [5] and a fast image acquisition time (2-3 seconds). With its high resolution and fast acquisition, HD-OCT could be a potential tool for precise analysis of the skin surface topography.

In the present work, we developed an automatic system to analyze skin images captured by HD-OCT and evaluated the skin surface topography using ISO standard roughness parameters. The computed parameters are then compared with the average subjective ranking score to evaluate the system's reliability. The proposed system is introduced in Section II, followed by the experimental results and a conclusion.

II. METHODS

A. *Overall System Framework*

The overall system framework as shown in Fig. 1 consists of two main steps namely, Skin Surface Detection and Skin Surface Topography Analysis & Measurement. The system will automatically process HD-OCT images of the skin, evaluate the skin surface roughness and generate the roughness parameter values.

B. *Skin Surface Detection*

The graph cut algorithm to segment the skin surface layer is defined as follows. In our method, we represent the pixels of

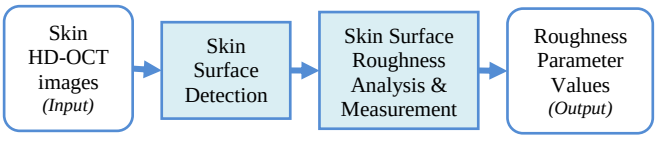

Figure 1. Overall System Framework

cross-sectional 2D HD-OCT image as a graph of nodes. The pixels (nodes) are connected through edges. As shown in Fig. 2, a weight value is assigned to each edge to represent the cost to path through the edge. To travel between nodes, the total cost will be the sum of all weight values assigned to the edges that connecting the nodes.

One of the main challenges for skin surface detection is the presence of hairs imaged during image acquisition, appearing as bright blobs floating above the skin surface on the image slices. This results in a shadow cast upon on the skin surface, weakening the contrast of the edge at the skin surface (Fig. 3). The strong edges of the hair may attract the pathing and lead to false detection of the skin surface boundary as shown in Fig. 3. Hence, the edges have to be assigned with appropriate weight values.

In this paper, we assign a high cost to non-edge pixels. We compute a mask M*(x, y)* where

$$M(x,y)\begin{cases}1 & 0 \le grad(x,y) < T \\ 0 & otherwise\end{cases} \quad (1)$$

The weight v(x, y) between two nodes is calculated based on the gradients at the nodes as follows:

$$v(x,y) = 2 - \text{grad}(x,y) - \text{grad}(x_n, y_n) + \lambda \cdot M(x,y) + \varepsilon \quad (2)$$

where grad*(x, y)* is the vertical gradient of the image at (*x*, *y*), grad(x_n, y_n) is the vertical gradient of the image at node (x_n, y_n), λ is a tuning parameter controlling the weight of the mask term, ε = 10-5 is the minimum weight in the graph added for system stabilization. In this paper, we set T equal to 3. From our test, the performance is not sensitive for very small T from 1 to 5. λ is a parameter which is set to a larger value such that the cost to pass by hair is high. In our experiments, λ is set at 100, which is not sensitive to the final performance as well.

Equation (2) assigns low weight values to node pairs with large vertical gradients. In our implementation, the gradients are normalized to values between 0 and 1. These weights are further adjusted to account for the directionality of the gradient. To segment the skin surface when is known that the boundary exhibits a dark to bright transition, we only calculate dark to bright gradient.

After assigning the weight values, graph search algorithm such as Dijkstra's algorithm [6] can be used to determine the finding the minimum path that connects the two endpoints.

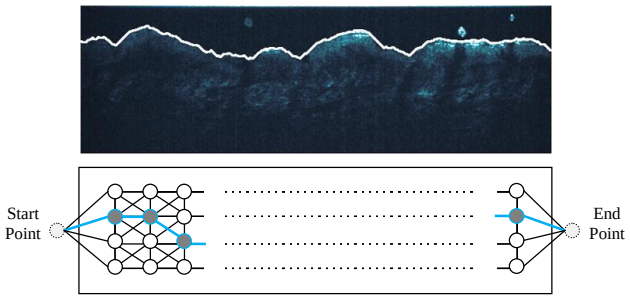

Figure 2. Detected skin surface (top), illustration of weight assigning to each edges to represent the cost to path though the edges (bottom)

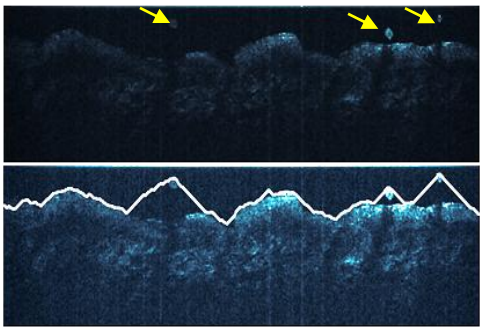

Figure 3. Orginal 2D HD-OCT image slice with hairs blobs (top), wrong skin surface surface boundary (bottom)

C. *Skin Surface Topography Analysis and Measurement*

Fig. 4 shows the process flow to achieve the roughness measurement. As skin surfaces are not of the same plane, segmented skin surfaces need to undergo a plane rectification process to correct the planes to a common plane. Based on the rectified skin surface, a depth map is generated. Skin HD-OCT images are captured using an imaging probe that produces *en face* images of size 640 × 512. However, there is a noticeable signal falloff at the edges of the imaging field of view. We observed that the signal within a circular region is of better quality compared to the signal outside the region. Hence, the size of the depth map is defined as 360 × 360, which is the maximum inscribed square to avoid noticeable signal falloff. The roughness measurement is then performed on the extracted depth map which provides the depth information for each pixel.

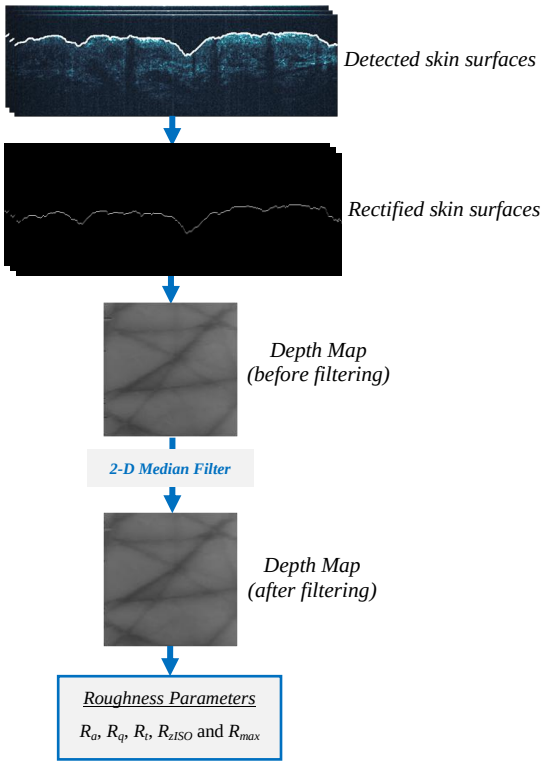

Figure 4. Process flow for Skin Surface Roughness Analysis and Measurement

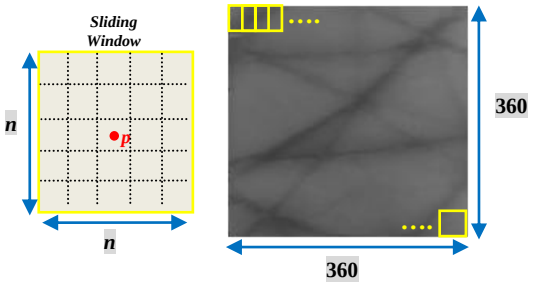

Figure 5. Sliding window of $n \times n$ is further divided into 25 patches for calculating R_{max} (left), Depth Map with sliding window *(right)*

As shown in Fig. 5, we proposed a sliding window approach on the 2D depth map to calculate the roughness. The sliding window is set to a size of $n \times n$, where the reference point, p is always at the center of the window. From the experimental results in Table I, the roughness measurement is not sensitive for window sizes of n = 20, 30 and 40.

In each window, we calculated the five roughness parameters and the computed results define the local values of R_a, R_q, R_t, R_{zISO} and R_{max} at p. In our work, the most commonly used roughness parameter R_a is defined as the average deviation of depth profile over each window area

$$R_a = \frac{1}{N}\sum_{n=1}^{N}|r_n| \tag{3}$$

where N is the number of pixels in the window and r_n is the topographic surface profile obtained from the surface segmentation. R_q is defined as the root-mean-square average roughness in each window and is calculated using Equation (4).

$$R_q = \sqrt{\frac{1}{N}\sum_{n=1}^{N} r_n^2} \tag{4}$$

The third roughness parameter R_t is defined as the sum of maximum depth value and minimum depth value in the window

$$R_t = \left|\max[r_n]\right| + \left|\min[r_n]\right| \tag{5}$$

R_{zISO} is a parameter that averages the sum of five highest peaks height and five deepest valleys depth over the evaluation length [7]. For our assessment, we calculated R_{zISO} in each window using Equation (6).

$$R_{zISO} = \frac{1}{5}\left(\sum_{n=1}^{5}\left|\max[r_n]\right| + \sum_{n=1}^{5}\left|\min[r_n]\right|\right) \tag{6}$$

The last roughness parameter R_{max} is an ISO parameter which serves a purpose similar to R_t. R_{max} finds the extreme peak-to-valley from five sampling lengths [7]. Within each window, we further subdivide the window into smaller patches. Each patch has a size of $n/5 \times n/5$ and R_t is calculated for each patch. Then, the highest R_t in the window is defined as the R_{max} for that window.

III. EXPERIMENTS AND RESULTS

We performed a human visual assessment experiment using HD-OCT skin images in 3-D form. A pool of HD-OCT healthy skin images (captured from cheeks, outer forearm and inner forearm) were grouped into three categories based on the roughness, with Category 1 having the smoothest surface and Category 3 having the roughest surface. Nine images were chosen randomly with each image from each of the three categories forming one set of test images as shown in Fig. 5.

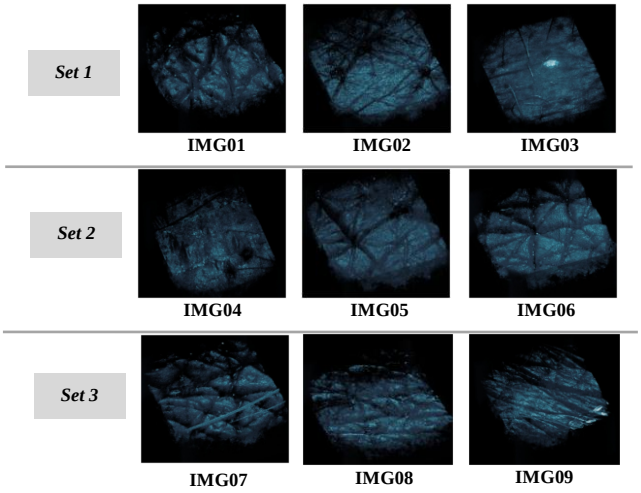

Figure 6. 9 test images divided into 3 sets, each set contains a image from all categories (Set 1: IMG01 from Category 3; IMG02 from Category 2; IMG03 from Catergory 1, Set 2: IMG04 from Category 1; IMG05 from Category 3; IMG06 from Catergory 2, Set 3: IMG07 from Category 3; IMG08 from Category 2; IMG09 from Catergory 1)

A total of 20 subjects participated in the evaluation of the appearance of skin roughness. Each subject was given the three sets of test images, which were printed on 70gsm paper. The subject was asked to rank the roughness of the three images in each set according to the roughness he or she perceived in normal viewing conditions.

There are three rankings (1, 2 and 3) with score 1 for the smoothest surface and 3 for the roughest surface perceived by the subjects. The ranking scores are analyzed and compared with the roughness parameters computed by our system. The results are shown in Table I. From the results, it can be seen that the computed values for all five parameters match in sequence with the average subjective ranking score.

In Table I, it is also observed that in Set 2, the average subjective ranking score for IMG05 and IMG06 (2.4 and 2.3 respectively) is close. However, the computed parameters showed a significant difference between the two test images. The 20 subjects have limited prior knowledge of skin surface analysis and almost half of them only consider the number of the furrows that they perceived as a guide when ranking the test images. On the other hand, the system evaluates the skin roughness based on the ISO amplitude parameters which considers the profile of skin surface topography instead of the number of furrows. From Fig. 6, it can be seen that IMG05 has darker lines which correspond to deeper furrows. In contrast, IMG06 has shallow furrows as the lines are lighter.

TABLE I. BJECTIVE TEST RESULTS AND COMPUTED ROUHNESS

Test Images		*Mean Subjective Ranking*	*n× n = 20 × 20*					*n× n = 30 × 30*					*n× n = 40 × 40*				
			R_a	R_q	R_t	R_{zISO}	R_{max}	R_a	R_q	R_t	R_{zISO}	R_{max}	R_a	R_q	R_t	R_{zISO}	R_{max}
Set 1	**IMG01**	3	2.72	3.29	14.30	13.52	4.61	3.59	4.32	19.24	18.49	6.69	4.33	5.21	23.41	22.68	8.63
	IMG02	2	1.11	1.37	6.55	6.05	2.83	1.31	1.63	8.42	7.91	3.78	1.49	1.86	10.12	9.59	4.60
	IMG03	1	0.80	1.02	5.17	4.67	2.40	0.93	1.18	6.63	6.10	3.13	1.05	1.33	7.92	7.37	3.77
Set 2	**IMG04**	1.3	0.95	1.18	5.80	5.32	2.59	1.13	1.41	7.46	6.98	3.39	1.30	1.62	9.01	8.51	4.08
	IMG05	2.4	2.82	3.40	14.90	14.05	5.12	3.71	4.46	19.85	19.05	7.32	4.47	5.37	24.04	23.25	9.40
	IMG06	2.3	1.97	2.38	10.57	9.92	3.68	2.56	3.09	14.12	13.49	5.19	3.06	3.70	17.27	16.65	6.61
Set 3	**IMG07**	3	2.81	3.42	15.36	14.45	5.31	3.68	4.47	20.76	19.88	7.71	4.43	5.38	25.42	14.45	5.31
	IMG08	1.75	2.40	2.91	13.21	12.34	4.71	3.14	3.79	17.58	16.75	6.69	3.78	4.56	21.30	12.34	4.71
	IMG09	1.25	2.06	2.52	11.31	10.60	3.66	2.67	3.25	14.98	14.31	5.38	3.16	3.84	18.04	10.60	3.66

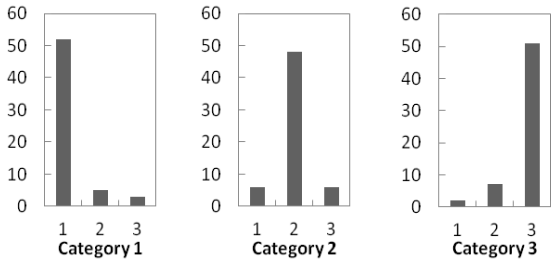

Figure 7. Distribution of ranking score in each category of roughness

The distribution of the subjective ranking scores for each category is shown in Fig. 7. The abscissa represents the three ranking scores (1, 2 and 3), and the coordinate shows the occurrence of the corresponding ranking score given by 20 subjects. Each of the 20 subjects is given three sets of test images. Hence, there are 60 scores in total for each category. From this figure, we can see that the subjective score ranking is comparable with the roughness parameters computed by the system.

IV. CONCLUSION

Current skin surface topography evaluation techniques such as replica-based methods have limitations which may result in errors and inaccurate measurements. The objective of our work is to develop an objective skin surface topography assessment tool using HD-OCT, a non-invasive skin image modality used clinically.

In this paper, we presented a system which automatically processes and analyzes HD-OCT skin images to evaluate the skin surface topography. The analysis uses the five most common amplitude parameters (R_a, R_q, R_t, R_{zISO} and R_{max}) of the International Organization for Standardization (ISO 4287:'97) as the skin roughness parameters. Experimental results show the computed amplitudes parameters match well with the mean ranking score obtained from subjective visual assessment. This work has proven the reliability of the developed system and the potential use of HD-OCT skin images for surface topography assessment. Such a system could be employed as an assessment tool in cases where follow-up methodology is treatment evaluation. It was also found that the variation of local window size does not affect the calculated roughness parameters. In this proposed system, we used the amplitude parameters for skin surface topography analysis and these parameters mainly depend on the depth of furrows. In future works, we will also analyze the frequency of irregularities in the skin surface topography and the widths of furrows which are also important when describing the skin surface.

ACKNOWLEDGMENT

This research work is a collaborative work between Institute for Infocomm Research, A*STAR and National Skin Centre, Singapore.

REFERENCES

[1] Lévêque, J.L. (1999), EEMCO guidance for the assessment of skin topography. Journal of the European Academy of Dermatology and Venereology, 12: 103–114. doi: 10.1111/j.1468-3083.1999.tb00998.x

[2] Takanori Igarashi , Ko Nishino , Shree K. Nayar, The Appearance of Human Skin: A Survey, Foundations and Trends® in Computer Graphics and Vision, v.3 n.1, p.1-95, January 2007

[3] Lioudmila Tchvialeva, Haishan Zeng, Igor Markhvida, David I McLean, Harvey Lui and Tim K Lee (2010). Skin Roughness Assessment, New Developments in Biomedical Engineering, Domenico Campolo (Ed.), ISBN: 978-953-7619-57-2, InTech

[4] Schmitz L, Reinhold U, Bierhoff E et al. Optical coherence tomography: its role in daily dermatological practice. J DtschDermatolGes. 2013 Jun; 11(6):499-507.

[5] Boone, Marc ALM, et al. High-definition optical coherence tomography imaging of melanocytic lesions: a pilot study. Archives of dermatological research (2013): 1-16.

[6] E. W. Dijkstra, A note on two problems in connexion with graphs. Numerische Mathematik 1(1), 269–271 (1959).

[7] Schreiner V, Sauermann G, Hoppe U, Characterisation of the skin surface by ISO-parameters for microtopography. In: Wilhelm KP, Elsner , Berardesca E and Maibach H, eds. Bioengineering of the skin: skin surface imaging and analysis. Boca Raton: CRC Press, 1997, 129-1